



Research Article

Experimental investigation of the impact of electronic expansion valve opening on vcr system performance: comparative analysis with capillary tube and thermostatic expansion valve

Ankitsinh CHAUHAN¹, Ashok PAREKH¹, Vimal PATEL^{1,*}

¹Department of Mechanical Engineering, S. V. National Institute of Technology, Surat 395007 Gujarat, India

ARTICLE INFO

Article history

Received: 21 May 2024

Revised: 29 August 2024

Accepted: 05 September 2024

Keywords:

VCR System, Expansion Devices, Performance Analysis of VCR System, Comparison of Expansion Devices, EXV Openings

ABSTRACT

The Electronic Expansion Valve controls the amount of refrigerant flow into the evaporator. The percentage opening of the electronic expansion valve significantly impacts the performance of the vapor compression refrigeration system as it controls the refrigerant flow to the evaporator which alters the superheating temperature and thus providing different cooling loads. In order to protect the compressor from damage from the liquid refrigerant, it is essential to vaporize all refrigerant before it leaves the evaporator. The experiments were conducted with an air-cooled condenser, a compressor frequency of 45 Hz, and a water pump frequency of 50 Hz. The experiments ran until the cold water temperature reached 10°C. R-134a refrigerant was used as the working fluid in all experiments. The conditions were kept similar for the capillary tube, thermostatic expansion valve, and electronic expansion valve. The performance parameters including cooling load, compressor power, and cooling coefficient of performance, were investigated by varying the electronic expansion valve percentage opening. The best performance achieved was that of a cooling load of 6560 W and COP of 4.56, with a 60% electronic expansion valve opening. In comparison to the capillary tube, the 60% electronic expansion valve opening provides an increase of 65% of the cooling load and increase of 39% of the coefficient of performance, respectively, and compared to thermostatic expansion valve, it provides an increase of 35% of the cooling load and increase of 10% of the coefficient of performance, respectively.

Cite this article as: Chauhan A, Parekh A, Patel V. Experimental investigation of the impact of electronic expansion valve opening on vcr system performance: comparative analysis with capillary tube and thermostatic expansion valve. J Ther Eng 2025;11(5):1468–1482.

INTRODUCTION

Air conditioning and refrigeration systems are increasingly prevalent in daily life, reflecting the rise in living standards in contemporary society. In Europe, heating

and cooling account for over half of all energy consumption [1]. Cooling and air conditioning systems currently represent approximately 20% of global energy consumption, and this share is projected to rise with the growing

*Corresponding author.

*E-mail address: vkp@med.svnit.ac.in

This paper was recommended for publication in revised form by Editor-in-Chief Ahmet Selim Dalkılıç



demand for cooling [2]. Consequently, there is a pressing need for energy-efficient technologies. Enhancing the efficiency of Vapor Compression Refrigeration (VCR) systems is crucial, and the expansion process plays a vital role in this improvement. In vapor compression refrigeration (VCR) systems, expansion devices are critical for regulating the flow and pressure of the refrigerant. These devices transform high-pressure, high-temperature refrigerant into a low-pressure, low-temperature state without the consumption of work [3]. Capillary tubes are the simplest form of refrigerant flow control, characterized by their design caused by the long and narrow tubes. These tubes are cost-effective and require a low starting torque [4]. The thermostatic expansion valve (TXV) is a vital component in HVAC systems and commercial refrigeration applications, particularly in walk-in coolers and freezers. Its main function is to precisely regulate the refrigerant flow into the evaporator coil by adjusting the flow passage opening, thereby controlling the refrigerant mass flow rate within the system. The TXV operates based on a suction superheat set point, calibrated to keep the refrigerant gas temperature above its saturation point at the compressor inlet [5-6]. Thermostatic expansion valves (TXV) can encounter difficulties in adjusting to substantial and quick changes in refrigerant flow, especially when variable-speed compressors are used. Traditional TXV, which are typically set to maintain a constant refrigerant flow rate under stable operating conditions, may require assistance to effectively respond to these dynamic changes [7]. In TXV-controlled direct expansion evaporator systems, hunting can occur under certain conditions where there are sustained oscillations in refrigerant flow rate, evaporating pressure, and superheat temperature [8].

Electronic expansion valves (EXV) are considered an alternative to TXVs for enhancing the performance of refrigeration systems in terms of operating efficiency and evaporator capacity. An EXV functions similarly to a TXV but employs a different control mechanism. Instead of relying solely on temperature sensing with a thermostatic element, an EXV compares the superheat level against a specified set point. This comparison generates a signal that regulates the opening or closing of the valve. The valve position is adjusted by a stepper motor controlled by a microprocessor. This electronic control system enables more precise and responsive regulation of refrigerant flow based on real-time superheat measurements. By continuously adjusting the valve opening according to the set superheat target, EXV can optimize system performance and efficiency, particularly in applications with variable operating conditions and load demands. The use of electronic control technology in EXV enhances the adaptability and effectiveness of refrigeration systems, providing improved reliability and energy efficiency compared to traditional TXV [9]. Many researchers believe that EXV offer superior control over superheat compared to TXV. Typically, TXV are set to maintain a degree of superheat between 5 to 8

°C under normal operating conditions. In contrast, EXV enable more efficient utilization of evaporator capacity by reducing the degree of superheat to approximately 3°C [10]. Thermostatic expansion valves (TXV) regulate the degree of superheat, but the stability of superheat can fluctuate if the control algorithm does not precisely adjust the valve's opening position. TXV usually employ proportional (P) control alone, lacking integral (I) control which is found in electronic expansion valves (EXV) equipped with proportional-integral-derivative (PID) control. EXV using PID control maintain more stable and precise superheat levels by incorporating integral control to correct deviations from the set point. This capability enhances the overall efficiency and effectiveness of refrigeration systems compared to traditional TXV [11]. Experimental analysis of an automotive air conditioning system with a thermostatic expansion valve (TXV) using two refrigerants, R-134a and R-1234yf, revealed that R-1234yf exhibited lower refrigeration capacity and COP compared to R-134a refrigerant [12]. The experimental results from the chiller system equipped with an EXV show a 30% reduction in superheat value and 6% lower power consumption compared to systems using TXVs. The control of superheat temperature in this setup utilizes a stepper control circuit with a fuzzy logic algorithm [13]. An examination of the refrigeration system with a variable speed compressor and different EXV openings reveals the use of a PI controller to regulate the EXV opening. The system maintains a superheat temperature of 6°C [14]. Many researchers have investigated various superheat temperature controllers, with studies employing fuzzy controllers [13, 15-16], predictive functional control (PFC) [17-19], and PI and PID controllers [20-23]. Among these, PID controllers are noted for providing superior control of superheat temperature compared to other types of controllers. Additionally, researchers have analyzed and modeled the adiabatic flow in capillary tubes for refrigerants such as R-22 and R-407C.

Many researchers have studied various configurations of EXV openings. It has been found that using an EXV consumes 9% less energy compared to a capillary tube in refrigerators [24]. Furthermore, a variable speed compressor paired with different EXV openings results in a chiller system with 30% lower superheat temperature and 6% lower power consumption compared to systems operated with TXV [13]. In the experimental study of a dual evaporation temperature-based chiller, it was observed that the cooling and heating capacity typically varies proportionally with compressor frequency. However, when considering the combination of EEV1 and EEV2 openings, there is an inverse relationship noted in the experimental results [25]. Additionally, researchers have conducted analysis and modeling of adiabatic flow in capillary tubes using refrigerants like R-22 and R-407C. The results of these models were compared with experimental data, demonstrating that the mathematical model yields optimal outcomes for air conditioning systems [26]. The numerical modeling

of a wire and tube condenser used in domestic refrigerators concluded that this modeling approach can be effectively utilized to design condensers for VCR systems [27]. An experimental investigation was conducted to enhance the performance of a domestic refrigerator by varying the length of the capillary tube (from 3.96 m to 5.18 m) with different combinations. The study concluded that the least energy consumption occurred with a capillary tube length of 4.3 m when using R-134a refrigerant [28].

Based on the literature reviewed, there is a limited number of studies focusing on enhancing the performance of Vapor Compression Refrigeration (VCR) systems. No specific experimental research has been conducted to investigate the performance of VCR systems using various openings of electronic expansion valves (EXV) at specific compressor frequencies. Current research trends suggest a shift towards adopting EXV to improve energy efficiency in refrigeration systems. PID controllers are favoured for their effectiveness in maintaining stable superheat temperatures. This study aims to investigate the performance of the VCR system by varying EXV openings and comparing them with other expansion devices such as capillary tubes and TXV under identical input parameters. The objective is to assess and compare the efficiency and effectiveness of these different expansion devices in VCR systems.

EXPERIMENTAL INVESTIGATION

Experimental Setup Description

The present study aims to investigate an experimental Variable Compression Refrigeration System (VCRS) with different Electronic Expansion Valve (EXV) openings and compare the performance using a capillary tube and TXV expansion devices. The experimental schematic diagram consists of the compressor, an air-cooled condenser (fin and tube), expansion devices (capillary tube, TXV, and EXV), and a plate heat exchanger that acts as the evaporator. Water from a 60-liter tank was circulated to the evaporator using a water flow pump. Various sensors were used, including RTD PT-100 temperature sensors, pressure transducers, a rotameter for refrigerant flow measurement, a paddle-wheel-type water flow meter, and humidity sensors. Data acquisition and control systems were integrated into a human-machine interface (HMI), facilitating seamless operation. Within the system, solenoid valves were used to control the equipment. A Eureka variable area glass tube rotameter, which provides $\pm 2\%$ accuracy over the flow range, was used to measure the refrigerant flow rate. The schematic diagram is shown in Figure 1.

The frequency of the semi-hermetic reciprocating variable speed compressor is regulated by a PLC (programmable logic controller). Suction and discharge pressure

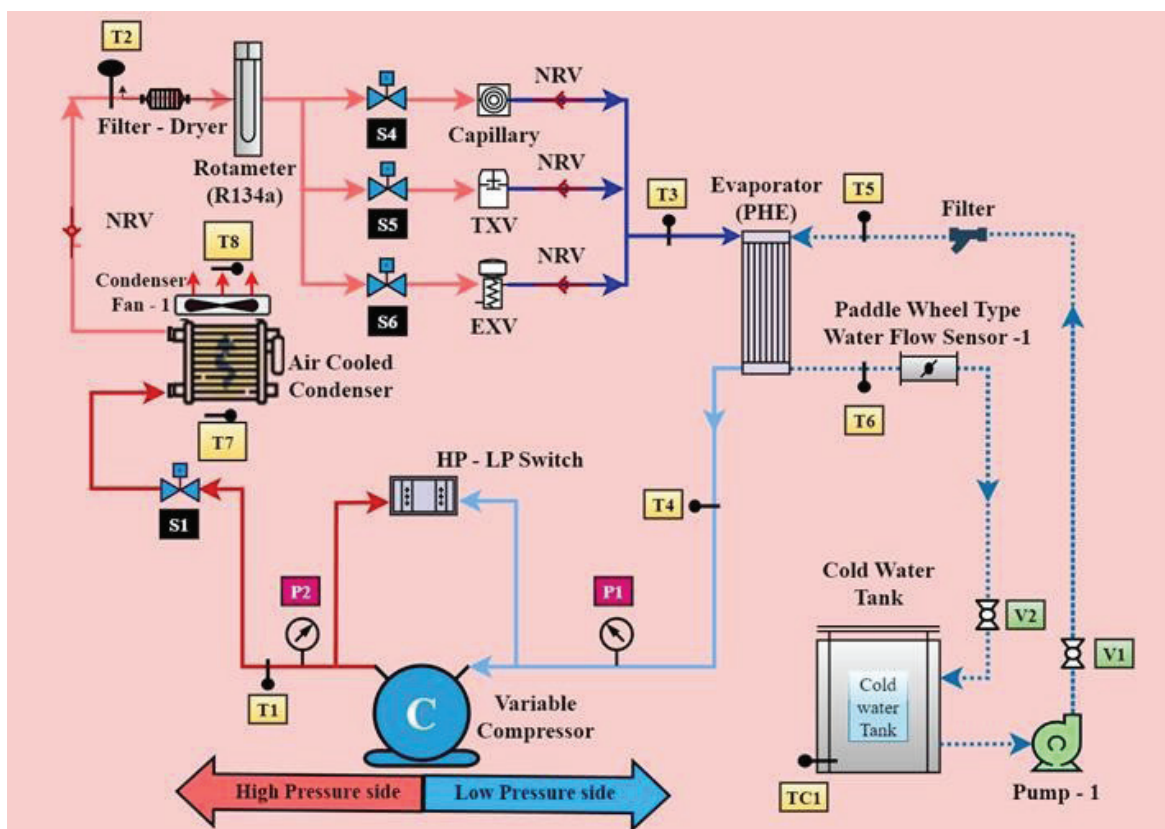


Figure 1. Schematic diagram of experimental setup.

transducers are installed to measure compressor pressure. Once compressed, the refrigerant R134a moves to an air-cooled fin and tube condenser. The refrigerant passes through a filter and then through a glass tube rotameter to measure the flow rate. Three types of expansion devices; thermostatic expansion valve (TXV), electronic expansion valve (EXV), and capillary tube are each controlled by their respective solenoid valves.

The water-cooled plate heat exchanger acts as an evaporator, with water circulated by a 60-liter stainless steel water tank using a PLC-controlled water pump. The flow rate of water is measured by a paddle wheel-type water flow meter, while the temperature is monitored using an RTD Pt 100 stainless steel sensor.

The RTD Pt 100 stainless steel sensors are installed to measure the inlet and outlet temperatures of the refrigerant at all four main components. Precisely, temperature sensors T1 measures the outlet and T4 measure the inlet temperature of the compressor respectively, T1 and T2 monitor those of the condenser, T2 and T3 measure the temperatures at the expansion device, and T3 and T4 measure the temperatures at the evaporator. The front view of the experimental setup, which includes the HMI screen, glass tube rotameter, and expansion devices with their respective solenoid valves, is depicted in Figure 2. The back view of the experimental setup, showcasing other components of the VCR system, is illustrated in Figure 3. The water-cooled and cooling tower based condenser is not used in present study.

The specifications of the different components of the VCR system are listed in Table 1. A semi-hermetic reciprocating compressor is used with refrigerant R134a, offering a capacity range of 0.75 to 1.25 tons of refrigeration (TR). The temperature of the refrigerant and water is measured using RTD Pt 100 stainless steel sensors, which provide

an accuracy of $\pm 0.1\%$ of full scale. Suction and discharge pressures are monitored using pressure transducers with an accuracy of $\pm 0.8\%$ of full scale. The measured data, including temperature, pressure, and water flow rate, is stored in the data acquisition system. The PLC controller regulates the Electronic Expansion Valve (EXV) opening.

Investigated Parameter

The performance of the VCR system is investigated with different expansion devices, including a capillary tube, thermostatic expansion valve (TXV), and various percentages of electronic expansion valve (EXV) openings (ranging from 30% to 70% in 5% increments). The following parameters are held constant for all experiments: compressor frequency set at 45 Hz, air-cooled fin and tube type condenser, water pump flow rate fixed at 50 Hz (23.1 LPM), initial water temperature in the evaporator tank maintained at 28°C, and the target cold water temperature set at 15°C. Measurements include the evaporative cooling tank's inlet and outlet water temperatures and different refrigerant temperatures at all four VCR components. Compressor power consumption is monitored using an energy meter. The cooling load, cooling COP, and system cooling COP are derived using mathematical equations.

Experimental Procedure

The experimental procedure commences by powering up the VCRES and configuring the desired parameters on the HMI screen, as specified in Table 2. It is crucial to allow a 30-minute stabilization period after making the selections on the HMI to achieve steady-state conditions within the system.

The initial water temperature in the evaporator tank is set at 28°C with a target temperature of 15°C. The compressor frequency is fixed at 45 Hz for all test runs. Data,



Figure 2. Front view of experimental setup.

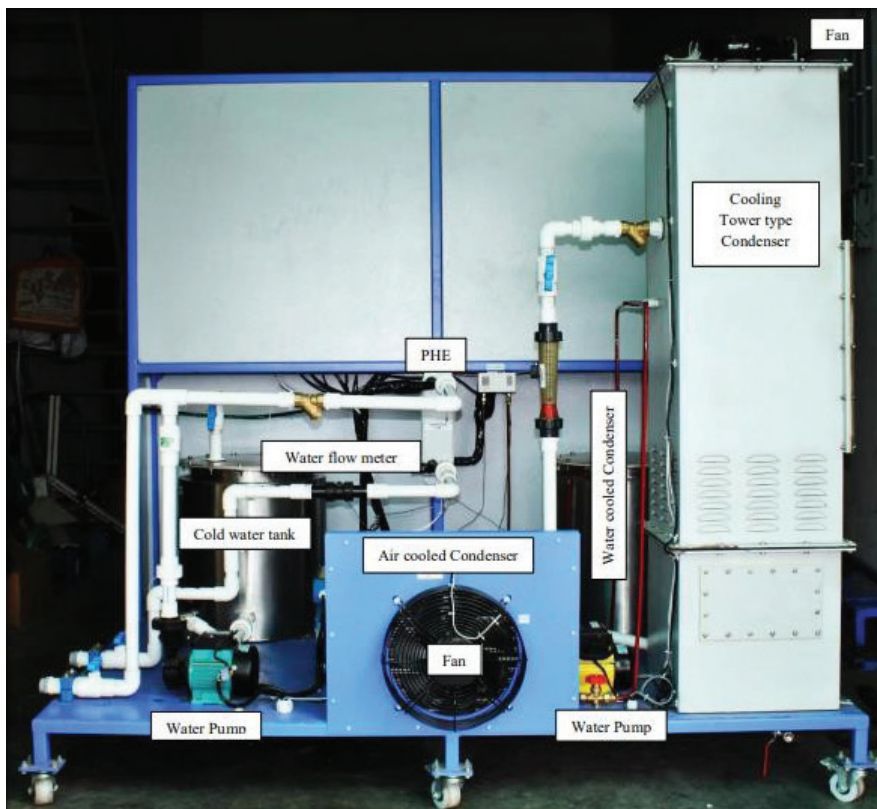


Figure 3. Back view of experimental setup.

Table 1. Specifications of different components

| Name of components | Description |
|---------------------------------|--|
| Compressor | Type: Semi-hermetic reciprocating Make: Frascold A1-6Y Refrigerant: R-134a Capacity: 0.75 – 1.25 TR, 400V, 30-60 Hz |
| Condenser | Type: Air cooled fin and tube |
| Expansion device | Type: Capillary tube, TXV and EXV |
| Evaporator | Type: Plate heat exchanger Suitable with most HFC, HFO and natural refrigerants. |
| Temperature sensor | Type: RTD Pt100, stainless steel sensor Accuracy: $\pm 0.1\%$ of full scale |
| Pressure transducers | Type: Sanhua YCQB Accuracy: $\pm 0.8\%$ full-scale |
| Water flow meter | Type: Peddle wheel Range: 20 – 50 lpm Accuracy: $\pm 4\%$ |
| R-134a flow meter | Type: Eureka PG-5 (Glass tube rotameter) Range: 15-140 lpm |
| Data acquisition & control unit | VFD drive, Water flow controller, PLC control and HMI |

Table 2. Input parameters of present experiment

| Parameter | Details |
|---|---|
| Compressor frequency (Hz) | 45 [25] |
| Condenser type | Air cooled fin and tube type with axial fan |
| Water pump flow rate (LPM) | 23.1 |
| Initial temperature of water in evaporator water tank ($^{\circ}\text{C}$) | 28 |
| Targeted cold water temperature in evaporator water tank ($^{\circ}\text{C}$) | 15 |
| EXV opening | 30% to 70% in the increment of 5%. |

including pressure, temperature, and water flow rate, are recorded and stored at 30-second intervals throughout the experiments until the water temperature reaches the target of 15°C. The recorded data is consistently saved in an Excel document during the experiment, facilitating subsequent performance measurements and analysis. The experiments are repeated for various EXV openings, ranging from 30% to 70% in 5% increments. Additionally, experiments are conducted using a capillary tube and TXV while keeping the same input parameters, and data are recorded for analysis purposes.

Mathematical Calculation

During the experiments conducted with the experimental setup, the temperature at the inlet and outlet of the evaporative cooling system is measured using the HMI system. The mass flow rates of water and refrigerant are measured using a paddle wheel-type flow meter and a rotameter, respectively. The compressor frequency is maintained at a constant 45 Hz throughout the experiment. Based on the data collected during these experiments, calculations are performed to determine the cooling load, cooling COP (Coefficient of Performance), and system cooling COP. The following is a brief description of these parameters:

Cooling load (Q_e)

The amount of heat absorbed per unit time by refrigerant in evaporator is termed as cooling load. It is calculated using Equation (1).

$$Q_e = \dot{m}_w * C_{pw} * (T_5 - T_6) \quad (1)$$

Cooling COP (COP)

The coefficient of performance (COP) describes the cooling capacity provided by compressor power. The cooling coefficient of performance is determined using Equation (2) as the ratio of the cooling load to work done by the compressor [29].

$$COP = \frac{Q_e}{W_c} \quad (2)$$

System cooling COP (COP_s)

A water pump facilitates water circulation in the chilled water tank, and an axial fan is used to flow air in a condenser. When calculating the system coefficient of performance (COP), it is essential to account for the power consumed by auxiliary devices. The total power (TP) of the system includes the power consumption of the water circulating pump, condenser axial fan, and compressor. Equation (3) provides the system cooling COP.

$$COP_s = \frac{Q_e}{TP} \quad (3)$$

Degree of superheating of refrigerant (ΔT_{sh})

The degree of superheating involves increasing the temperature of a vapor refrigerant above its saturation

temperature. Superheating is quantified as the temperature difference between the actual vapor and saturation temperatures corresponding to the refrigerant's pressure. It is determined by measuring the pressure and temperature, determining the saturation temperature, and calculating the difference. The superheating temperature is computed using Equation (4).

$$\Delta T_{sh} = T_{act} - T_{sat} \quad (4)$$

Where; T_{act} is an actual temperature of vapour and T_{sat} is a saturated temperature of refrigerant

RESULTS AND DISCUSSION

During the experiment, data collection was conducted at regular 60-second intervals. Various primary parameters, including pressures, temperatures, and flow rates, were measured and recorded. The experiments continued until the water temperature in the cold-water tank reached the desired temperature of 15 °C. The effects on various parameters are discussed in detail in the following paragraphs.

Compressor Discharge Temperature and Pressure Ratio

The Electronic Expansion Valve (EXV) regulates refrigerant flow into the evaporator coil based on the system's demands. The refrigerant flow rate increases when the EXV opens more comprehensively, allowing more refrigerant to enter the evaporator. Consequently, the pressure ratio also decreases. Essentially, as the EXV opens further, permitting more refrigerant to flow through the evaporator its pressure rises. The variation of pressure ratio at different valve opening is shown in Figure 4.

The increase in evaporator pressure subsequently increases the suction pressure at the compressor inlet. The compressor requires more work to achieve the desired discharge pressure when operating under increased suction pressure due to the broader EXV opening, because the overall work required is increased majorly due to higher mass flow rate. The initial refrigerant flow rate and compression workload may increase when the refrigeration system starts operating. This results in an initial rise in discharge temperature as the compressor compresses the incoming refrigerant to achieve the desired pressure and temperature conditions. The compressor may generate more heat during this phase, leading to a higher discharge temperature. As the system stabilizes and reaches a steady-state condition, the discharge temperature increases until it reaches a peak value. Then, the compressor adjusts to the required refrigeration load, stabilizing the refrigerant flow rate. As a result, the compressor operates more efficiently with reduced heat generation, gradually reducing and stabilizing the discharge temperature over time. Figure 5 illustrates the variation in compressor discharge temperature.

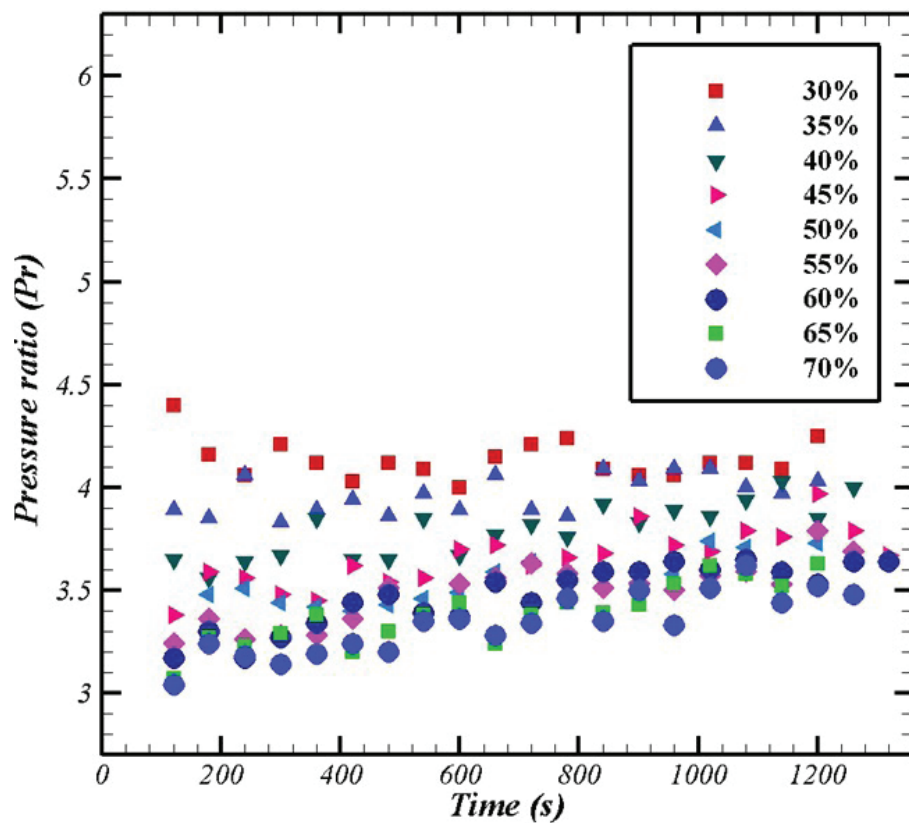


Figure 4. Effect on pressure ratio of EXV opening.

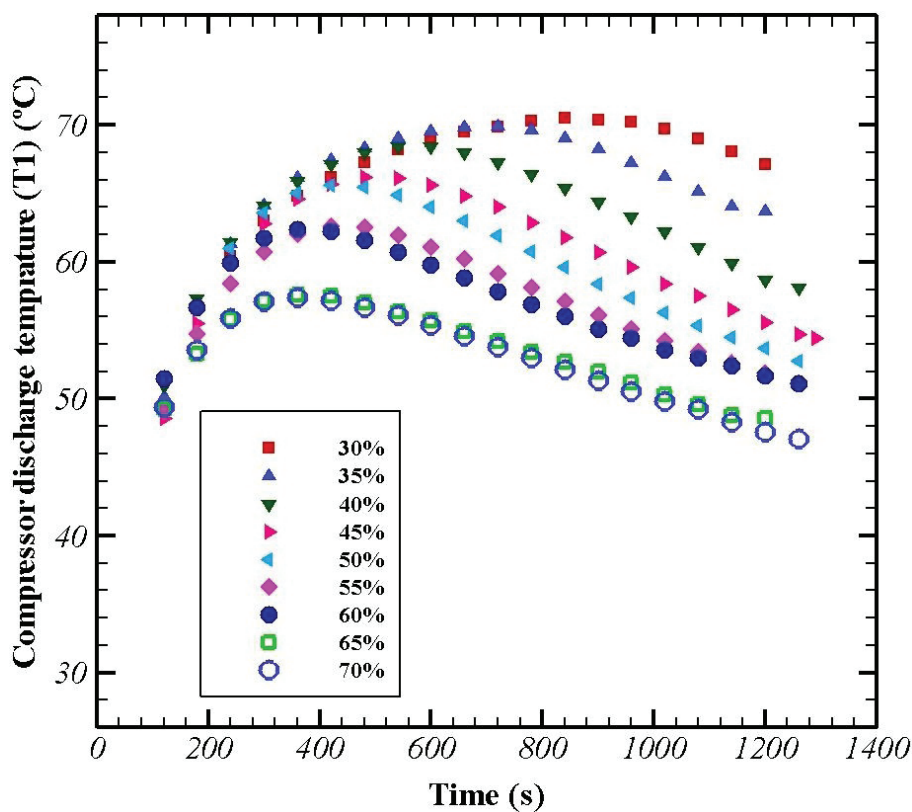


Figure 5. Effect on compressor discharge temperature of EXV openings.

Superheating of Refrigerant

With increase in EXV opening (increased refrigerant flow rate) corresponds to an increase in evaporator pressure, which reduces the refrigerant's saturation temperature within the evaporator coil. When the EXV opening is increased from 30% to 70%, there may be a transient period where system parameters, including superheat temperature, undergo rapid changes. The superheat temperature may initially decrease sharply as the EXV allows more refrigerant into the evaporator, leading to lower evaporator temperatures. As the system stabilizes with the wider EXV opening, the superheat temperature reaches a new equilibrium level. The reduction in superheat temperature becomes more gradual and stabilizes at a lower value compared to the initial conditions.

With lower EXV opening the inlet temperature of evaporator is low with lower evaporator pressure, this results in more sensible heat transfer to the vapor phase resulting in high superheating temperature. As the EXV opening is increased, the liquid fraction is increased along with increase in pressure in the flow, which gives lower superheating temperature due to latent of vaporisation. However, on further opening the EXV increase in pressure dominates thus reducing the saturation temperature and increasing the superheating temperature. Effect of EXV opening on superheating temperature is shown in Figure 6.

Condenser outlet temperature

The condenser outlet temperature in a vapor compression refrigeration system refers to the temperature of the refrigerant leaving the condenser. It plays a crucial role in the overall system performance and efficiency. The condenser's primary function is to remove heat from the refrigerant and reject it to the surrounding environment. The condenser outlet temperature reflects the effectiveness of this heat rejection process. A higher condenser outlet temperature indicates that the refrigerant is not being adequately cooled, and the heat transfer process is less efficient. The condenser outlet temperature is closely related to the refrigerant's saturation pressure. As the condenser outlet temperature increases, the saturation pressure of the refrigerant also tends to increase. The outlet temperature of the condenser observed over time typically exhibits dynamics influenced by system operation and external factors. Initially, the condenser outlet temperature may show fluctuations as the system stabilizes, adjusting to varying load conditions or EXV settings. Over time, as the system reaches steady-state operation, the condenser outlet temperature tends to stabilize within a specific range, reflecting consistent heat rejection performance. Factors such as ambient conditions, system load variations, and EXV control adjustments can influence the long-term trend of the condenser outlet temperature. The effect of EXV opening on condenser outlet temperature is shown in Figure 7.

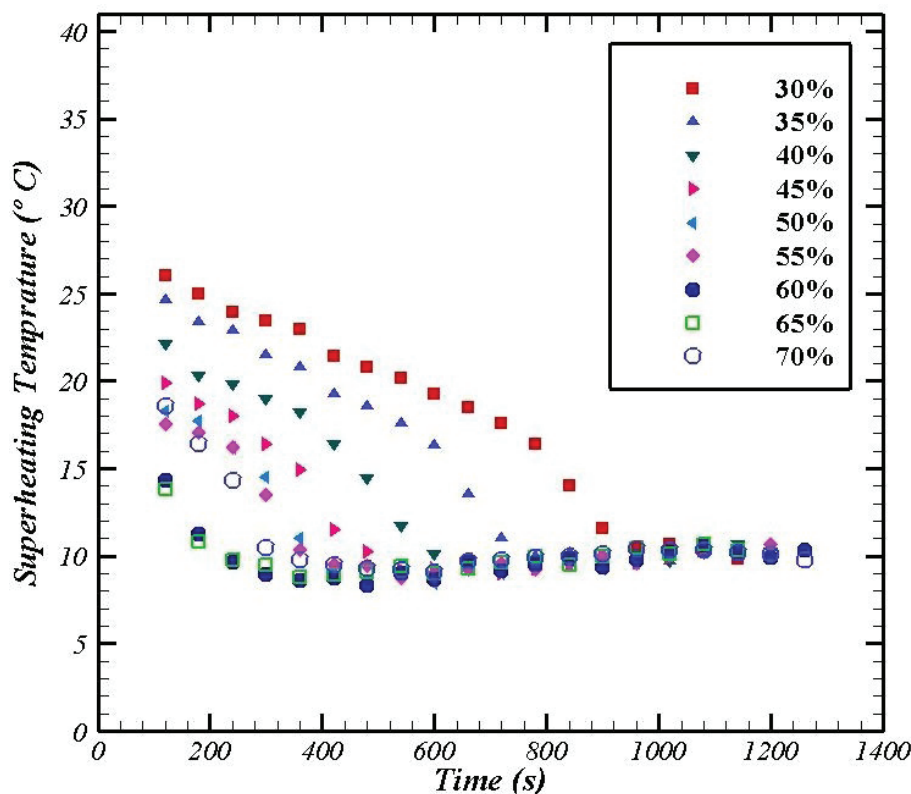


Figure 6. Effect on degree of superheating of EXV opening.

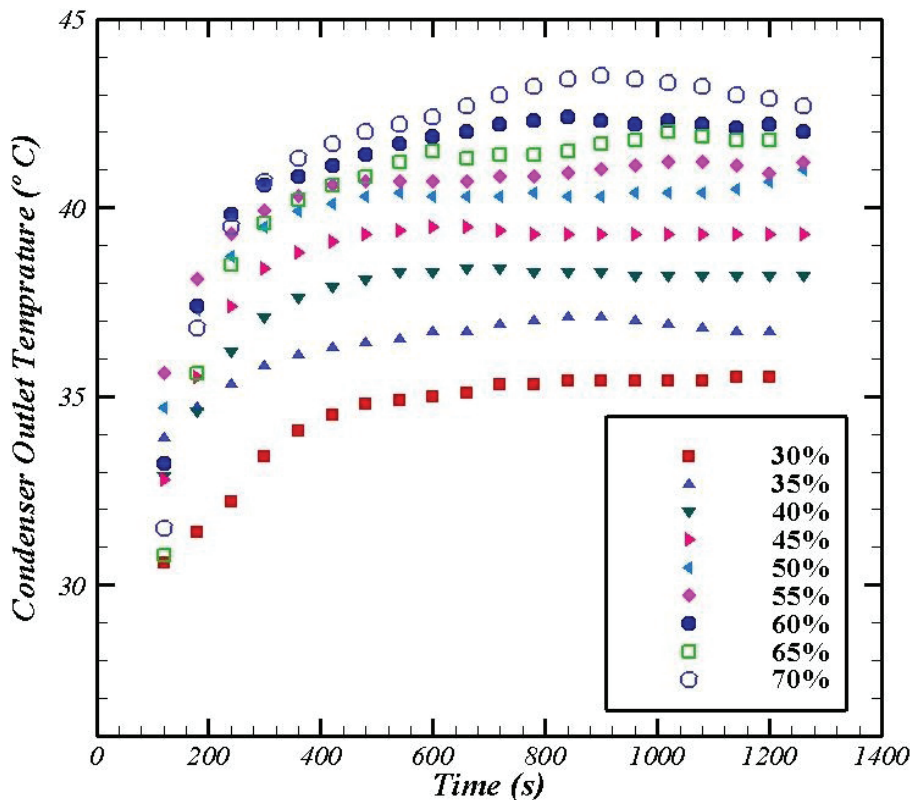


Figure 7. Effect on condenser outlet temperature of EXV opening.

Cooling load (Q_c)

The data reveals a clear trend in the relationship between EXV opening and cooling load in the refrigeration system. Initially, as the EXV opening increases from 30% to 60%, there is a substantial and proportional increase in cooling load. Specifically, the average cooling load at a 60% EXV opening is significantly higher compared to lower openings, with a 22.58% more compared to a 30% opening and a 20.15% higher compared to a 35% opening. This demonstrates that widening the EXV opening up to 60% allows for a more substantial refrigerant flow, leading to enhanced heat transfer and greater cooling capacity. Beyond an EXV opening of 60%, the cooling load continues to increase but at a diminishing rate, as indicated by the smaller percentage increases at 65% (3.4% increase) and 70% (6.1% increase) EXV openings. This diminishing return suggests that beyond a certain point (around 60% opening), additional increases in the EXV opening yield relatively smaller gains in cooling load. Therefore, the optimal EXV opening for maximizing cooling load efficiency is around 60%, highlighting the importance of careful EXV control to achieve optimal system performance and efficiency. Effect of EXV opening on cooling load is shown in Figure 8.

Compressor Work (W_c)

The electronic expansion valve's (EXV) opening position significantly impacts the compressor's performance

in a refrigeration system. The EXV opening directly affects the pressure and mass flow rate of the refrigerant entering the compressor, affecting the compressor's workload. As the EXV opening increases, the pressure at the compressor inlet increases, resulting in a lower compression ratio. This decrease in compression ratio reduces the work required by the compressor per unit mass, as it operates at a lower pressure and temperature. However, with further increases in the EXV opening, the mass flow rate of refrigerant entering the compressor also increases. Consequently, the compressor must work harder to accommodate the higher refrigerant flow rate. This higher flow rate requires the compressor to perform more work to compress the larger refrigerant volume, leading to an initial increase in compressor work. As the refrigerant flow rate continues to increase and reaches a point where the compressor's capacity is maximized, further increases in flow rate do not proportionally increase the compressor's workload. This results in an initial rise in power consumption. As mentioned above, on further increasing the EXV opening beyond a certain threshold, the decrease in pressure ratio dominates the mass flow rate of the refrigerant. As a result, the compressor's power consumption decreases, leading to the observed declining trend in power consumption with wider EXV openings.

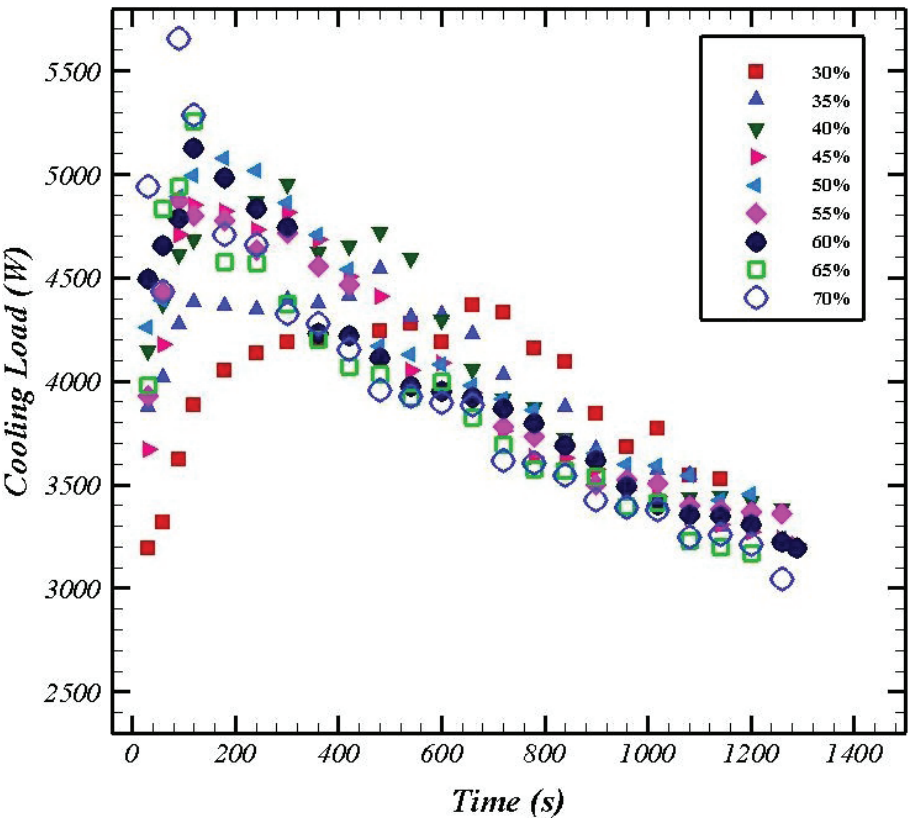


Figure 8. Cooling load for different EXV opening.

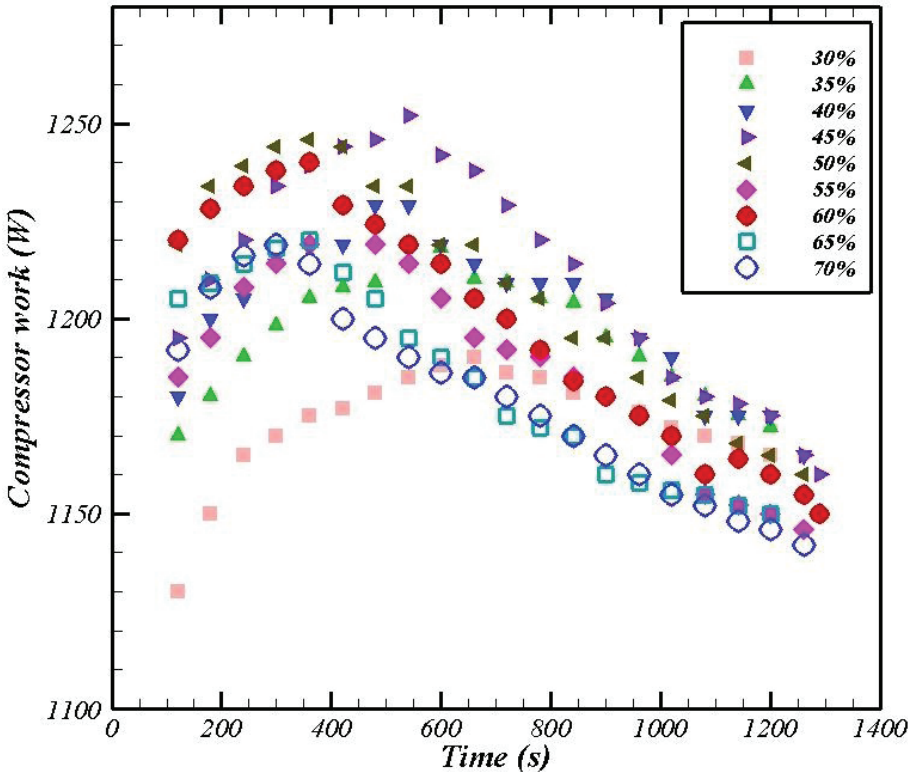


Figure 9. Compressor work for different EXV opening.

Cooling COP (COP_C)

The coefficient of performance (COP) in a refrigeration system, which quantifies heat transfer efficiency, is significantly influenced by the opening position of the electronic expansion valve (EXV). As the EXV opening increases, the cooling load also tends to rise due to the higher mass flow rate of refrigerant entering the evaporator, reaching its peak efficiency at around 60% EXV opening. However, further widening of the EXV opening results in increased compressor power consumption beyond this optimal point. This occurs because the compressor must handle a larger refrigerant volume at higher flow rates, leading to elevated workload and energy consumption. Consequently, the COP begins to decline for EXV openings of 65% and 70% compared to the optimal 60% opening. The observed trend highlights the trade-off between cooling performance and energy efficiency, emphasizing the importance of selecting an EXV opening that maximizes COP by effectively

balancing cooling load and compressor power consumption. The average COP for 60% of openings is 19% higher than for 30 and 35% of openings of EXV and 10% higher than for 40, 45 and 50% of EXV openings. The average COP for 65 and 70% opening is 1% and 5% lower than 60% of EXV opening. The effect of EXV opening on cooling COP of system is shown in Figure 10.

Validation

For validation, the experimental data compared with the theoretical calculation use of data provided by CoolPack software. The software works on engineering equation solver (EES). The input conditions are taken from the recorded data of the experiments. The percentage error is below 5% in the all cases. Table 3 shows the validation of experimental data with theoretical data.

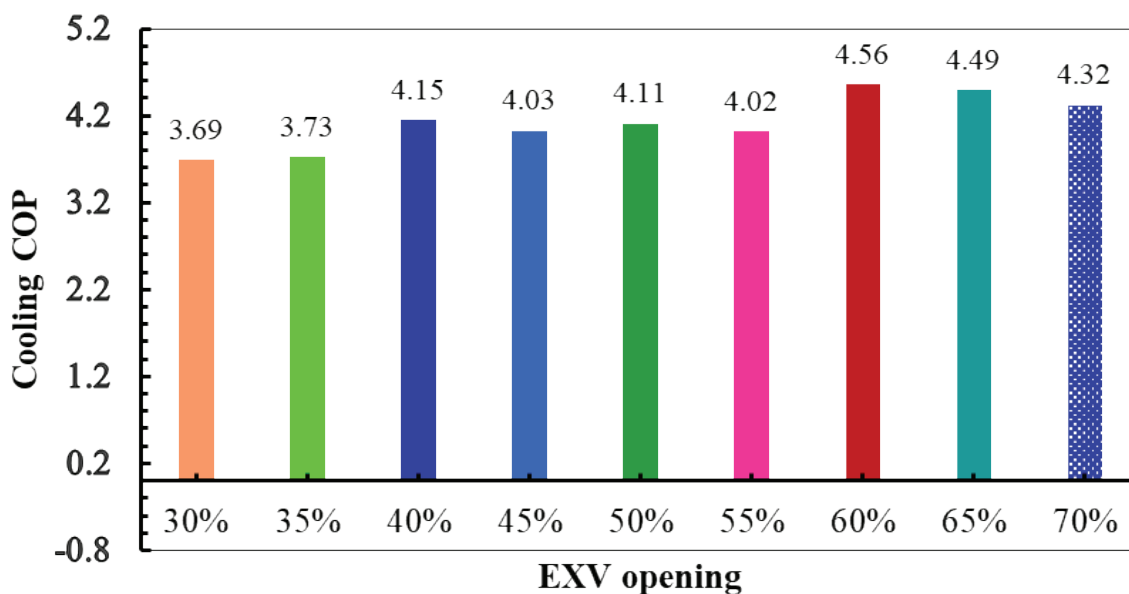


Figure 10. Cooling COP for different EXV opening.

Table 3. Validation of experimental data with theoretical data

| EXV opening | Cooling COP (Experimental) | Cooling COP (Theoretical) | % Error |
|-------------|----------------------------|---------------------------|---------|
| 30 | 3.69 | 3.52 | 4.6 |
| 35 | 3.73 | 3.79 | 1.6 |
| 40 | 4.15 | 4.26 | 2.6 |
| 45 | 4.03 | 4.21 | 4.4 |
| 50 | 4.11 | 4.07 | 0.9 |
| 55 | 4.02 | 4.11 | 2.2 |
| 60 | 4.56 | 4.69 | 2.8 |
| 65 | 4.49 | 4.53 | 0.9 |
| 70 | 4.32 | 4.52 | 4.6 |

COMPARISON OF CAPILLARY, TXV AND EXV

All experimental work was conducted under similar input conditions for the capillary tube, thermostatic expansion valve (TXV), and electronic expansion valve (EXV), as detailed in Table 2. Figure 11 compares compressor power consumption, cooling load, and cooling coefficient of performance (COP) for these expansion devices. The results indicate that the cooling load achieved with the EXV is higher than that of the TXV and capillary tube. Specifically,

at a 60% EXV opening, the cooling load is 65% and 35% greater than that of the capillary tube and TXV, respectively. Additionally, the compressor requires more power due to higher superheat temperatures associated with the EXV compared to the TXV. Despite this, the cooling load achieved with the EXV remains significantly higher than that of the TXV and capillary tube, with relatively minimal changes in power consumption between the EXV and capillary tube. Consequently, the cooling COP of the EXV (at 60% opening) exceeds that of the capillary tube and TXV by

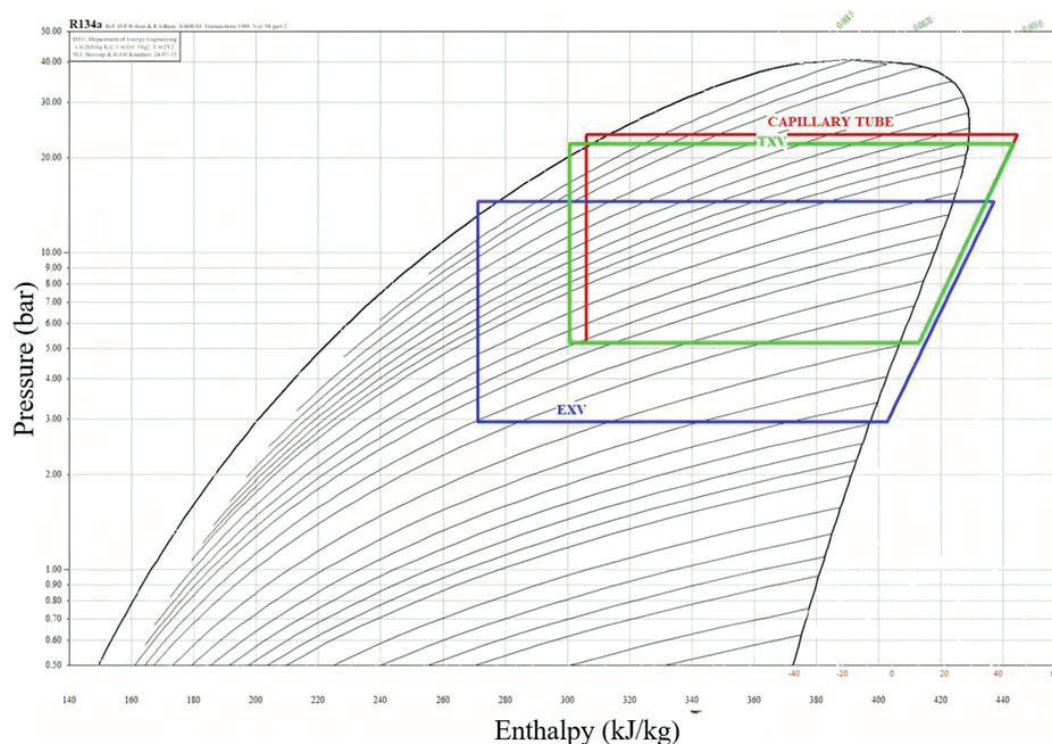


Figure 11. P-h diagram of expansion devices used.

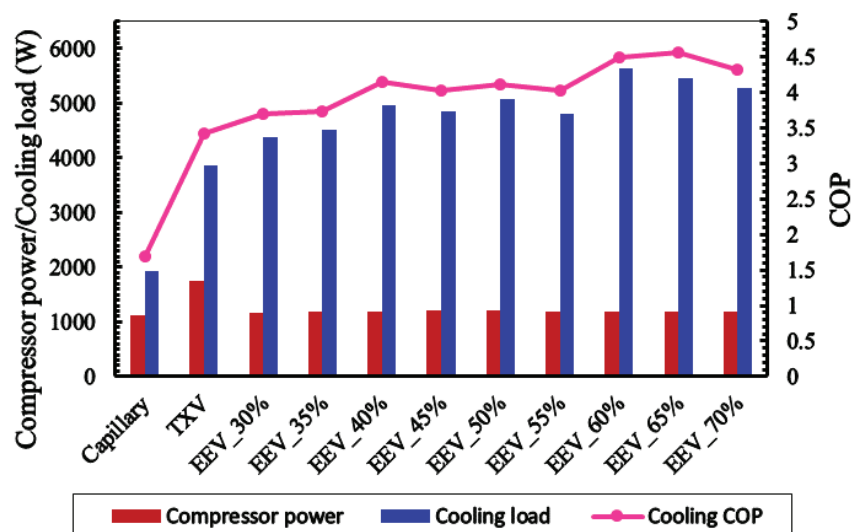


Figure 12. Comparison of performance for different expansion devices.

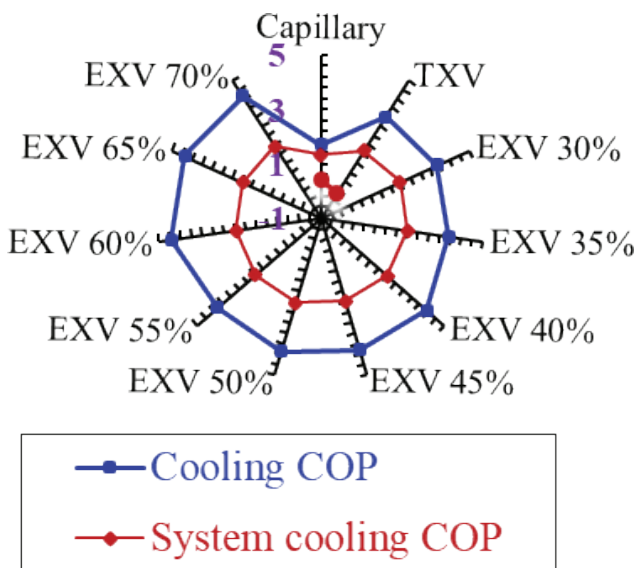


Figure 13. Comparison of performance for different expansion devices.

39% and 10%, respectively. The comparison of performance for different expansion devices is shown in Figure 12.

The pressure enthalpy diagram of VCR system with capillary tube, TXV and EXV expansion devices is shown in Figure 11.

The cooling COP and system cooling COP for capillary tube, TXV, and EXV are plotted on the radar graph and shown in Figure 13. The COP of the system is defined as the ratio of cooling load to total power consumed by the system. The total power (TP) of the system includes the power consumption of the water circulating pump, condenser axial fan, and compressor. The maximum cooling COP achieved is 4.56 for EXV opening of 60% which is 39% and 10% higher than capillary and TXV respectively.

CONCLUSION

The performance of the VCR system was investigated using various expansion devices, including a capillary tube, a thermostatic expansion valve (TXV), and an electronic expansion valve (EXV) at different opening percentages ranging from 30% to 70% in 5% increments. The experiments were conducted at a compressor frequency of 45 Hz. As the EXV opening increased from 30% to 70%, the discharge temperature and pressure ratio decreased, resulting in improved cooling efficiency and reduced compressor power consumption. This significant reduction in superheat temperature, attributed to the higher refrigerant flow rate associated with wider EXV openings, contributed to enhanced cooling rates and overall system performance. However, it is noteworthy that the condenser outlet temperature increased as the EXV opening widened, suggesting

that a broader EXV opening may lead to less effective heat rejection and lower system efficiency.

1. The maximum cooling load of 6560 W is achieved at a 60% EXV opening. At a 60% EXV opening, the cooling load was 22.58% higher compared to a 30% opening and 20.15% higher compared to a 35% opening.
2. The cooling load remained consistently higher, increasing by around 10 to 12%, in the EXV opening range of 40% to 55%. However, for EXV openings of 60% and higher, the cooling load exhibited diminishing returns, with a minor increase of 3.4% for a 65% EXV opening and a 6.1% increase for a 70% EXV opening.
3. The highest COP value is achieved at a 60% EXV opening, with a 19% increase compared to a 30% and 35% EXV opening and a 10% increase compared to a 40%, 45%, and 50% EXV opening.
4. The COP for 65% and 70% EXV openings was slightly lower, with a 1% and 5% decrease, respectively, compared to the 60% EXV opening.
5. The cooling COP of the EXV (at 60% opening) was 39% and 10% higher compared to the capillary tube and TXV.

NOMENCLATURES

| | |
|-----------|--|
| C_{pw} | Specific heat of water (J/kg.K) |
| m_w | Mass flow rate of water (kg/s) |
| Q_e | Cooling load (W) |
| T_1 | Compressor discharge temperature of refrigerant (°C) |
| T_2 | Condenser outlet temperature of refrigerant (°C) |
| T_3 | Evaporator inlet temperature of refrigerant (°C) |
| T_4 | Compressor suction temperature of refrigerant (°C) |
| T_5 | Inlet temperature of water of evaporator (°C) |
| T_6 | Outlet temperature of water of evaporator (°C) |
| TC_1 | Cold water tank controlling temperature (°C) |
| T_{10} | Air cooled condenser air outlet temperature (°C) |
| T_{sat} | Refrigerant saturated temperature (°C) |
| T_{act} | Refrigerant actual temperature (°C) |
| T_{sh} | Degree of superheating °C |
| TP | Total power (W) |
| WC | Compressor work (W) |

Abbreviations

| | |
|------|---|
| CCD | Central composite design |
| COP | Cooling coefficient of performance |
| COPS | System cooling coefficient of performance |
| DF | Degree of freedom |
| EXV | Electronic expansion valve |
| HFC | Hydro-fluorocarbons |
| HFO | Hydro-fluoroolefin |
| HMI | Human Machine Interface |
| HVAC | Heating ventilation and air conditioning |
| LPM | Liters per minutes |
| PHE | Plate heat exchanger |
| PF | Proportional-Fuzzy |
| PI | Proportional-Integral |
| PID | Proportional-Integral-Derivative |

| | |
|------|---|
| PLC | programmable logic controller |
| RSM | Response surface method |
| TXV | Thermostatic expansion valve |
| VCRS | Vapour compression refrigeration system |
| VFD | Variable frequency drive |

Subscripts

| | |
|------|--------------|
| act. | Actual |
| c | Compressor |
| s | System |
| sat. | Saturated |
| sc | Subcooling |
| sh | Superheating |
| w | Water |

ACKNOWLEDGEMENT

I sincerely thank Sardar Vallabhbhai National Institute of Technology (SVNIT), Surat, for providing the necessary laboratory facilities and resources for this project. The support and infrastructure made available greatly contributed to the successful completion of my work. I would like to extend my heartfelt gratitude to Ishant Patil and Nachiket Shah for their invaluable assistance in conducting the experiments. Their dedication, hard work, and keen insight were instrumental in the successful completion of this research. Thank you for your unwavering support and contributions.

AUTHORSHIP CONTRIBUTIONS

Authors equally contributed to this work.

DATA AVAILABILITY STATEMENT

The authors confirm that the data that supports the findings of this study are available within the article. Raw data that support the finding of this study are available from the corresponding author, upon reasonable request.

CONFLICT OF INTEREST

The author declared no potential conflicts of interest with respect to the research, authorship, and/or publication of this article.

ETHICS

There are no ethical issues with the publication of this manuscript.

STATEMENT ON THE USE OF ARTIFICIAL INTELLIGENCE

Artificial intelligence was not used in the preparation of the article

REFERENCES

- [1] Urchueguía JF, Alakangas E, Berre I, Cabeza LF, Grammelis P, Haslinger W, van Helden W. Common implementation roadmap for renewable heating and cooling technologies: European Technology Platform on Renewable Heating and Cooling 2014.
- [2] Dupont JL, Domanski P, Lebrun P, Ziegler F. The role of refrigeration in the global economy. Informatory Note on Refrigeration Technologies 2019.
- [3] Cengel YA, Boles MA, Kanoğlu M. Thermodynamics: an engineering approach. New York (NY): McGraw-Hill; 2011. p. 445.
- [4] Zhang CL. Generalized correlation of refrigerant mass flow rate through adiabatic capillary tubes using artificial neural network. Int J Refrigeration. 2005;28:506-514. [\[Crossref\]](#)
- [5] Wichman A, Braun JE. Fault detection and diagnostics for commercial coolers and freezers. HVAC&R Res 2009;15:77-99. [\[Crossref\]](#)
- [6] ASHRAE A. Advanced Energy Design Guide for K-12 School Buildings: Achieving 30% energy savings toward a net zero energy building, W Stephen Comstock. [place unknown]: ASHRAE; 2008.
- [7] Chen W, Zhijiu C, Ruiqi Z, Yezheng W. Experimental investigation of a minimum stable superheat control system of an evaporator. Int J Refrigeration 2002;25:1137-1142. [\[Crossref\]](#)
- [8] Mithraratne P, Wijesundera NE. An experimental and numerical study of hunting in thermostatic-expansion-valve-controlled evaporators. Int J Refrigeration 2002;25:992-998. [\[Crossref\]](#)
- [9] Yu FW, Chan KT, Chu HY. Constraints of using thermostatic expansion valves to operate air-cooled chillers at lower condensing temperatures. Appl Thermal Eng 2006;26:2470-2478. [\[Crossref\]](#)
- [10] Roper, M. A. (2000). Energy efficient chiller control. BSRIA
- [11] Finn DP, Doyle CJ. Control and optimization issues associated with algorithm-controlled refrigerant throttling devices. Univ Coll of Dublin (IE); 2000.
- [12] Alkan A, Kolip A, Hosoz M. Energetic and exergetic performance comparison of an experimental automotive air conditioning system using refrigerants R1234yf and R134a. J Therm Eng 2021;7:1163-1173. [\[Crossref\]](#)
- [13] Ekren O. Energetic assessment of an electronic and a thermostatic expansion valve for a variable capacity compressor. J Adv Therm Sci Res 2019;6:51-57. [\[Crossref\]](#)
- [14] Li H, Jeong SK, You SS. Feedforward control of capacity and superheat for a variable speed refrigeration system. Appl Thermal Eng 2009;29:1067-1074. [\[Crossref\]](#)
- [15] Chia PK, Tso CP, Jolly PG, Wong YW, Jia X. Fuzzy control of superheat in container refrigeration using an electronic expansion valve. HVAC&R Res 1997;3:81-98. [\[Crossref\]](#)

- [16] Shuai Y, Wen M, Wen X, Li Z, P Shao-fei. Fuzzy control application of electronic expansion valve regulation in heat pump system. *Autom Instrum* 2016;6:13.
- [17] Changenet C, Charvet JN, Gehin D, Sicard F, Charmel B. Study on predictive functional control of an expansion valve for controlling the evaporator superheat. *Proc Inst Mech Eng Part I J Syst Control Eng* 2008;222:571-582. [\[Crossref\]](#)
- [18] Fallahsohi H, Changenet C, Placé S, Ligeret C, Lin-Shi X. Predictive functional control of an expansion valve for minimizing the superheat of an evaporator. *Int J Refrigeration* 2010;33:409-418. [\[Crossref\]](#)
- [19] Saleh B, Aly AA. Flow control methods in refrigeration systems: A. *Int J Control Autom Syst* 2015;4.
- [20] Maia AAT, Silva MDA, Koury RNN, Machado L, Eduardo AC. Control of an electronic expansion valve using an adaptive PID controller.
- [21] Tesfay M, Alsaleem F, Arunasalam P, Rao A. Adaptive-model predictive control of electronic expansion valves with adjustable setpoint for evaporator superheat minimization. *Build Environ* 2018;133:151-160. [\[Crossref\]](#)
- [22] Rasmussen H, Thybo C, Larsen LFS. Nonlinear superheat and evaporation temperature control of a refrigeration plant. *IFAC Proc Vol* 2006;39:251-254. [\[Crossref\]](#)
- [23] Al-Badri AR, Al-Hassani AH. A control method using adaptive setting of electronic expansion valve for water chiller systems equipped with variable speed compressors. *Int J Refrigeration* 2020;119:102-109. [\[Crossref\]](#)
- [24] Knabben FT, Ronzoni AF, Hermes CJ. Application of electronic expansion valves in domestic refrigerators. *Int J Refrigeration* 2020;119:227-237. [\[Crossref\]](#)
- [25] Li R, Zhu Y, Yang Y, Li K, Zhang R, Sun J, Sun Z. The effects of the opening of the electronic expansion valve in the high-stage cycle on the performance of a cascade heat pump water heater. *J Build Eng* 2021;42:103015. [\[Crossref\]](#)
- [26] Imran AA. Adiabatic and separated flow of R-22 and R-407C in capillary tube. *Eng Tech J* 2009;27. [\[Crossref\]](#)
- [27] Imran AA, Jafal HM. Numerical modeling of wire and tube condenser used in domestic refrigerators. *J Eng Sustain Dev* 2009;13:1-17.
- [28] Gugulothu S. Enhancement of household refrigerator energy efficiency by studying the effect of refrigerant charge and capillary tube length. *J Therm Eng* 2021;7:1121-1129. [\[Crossref\]](#)
- [29] Selloum A, Triki Z, Chiba Y. Thermodynamic analysis of a solar-driven vapor compression refrigeration system using R1234ze for cooling applications in Ghardaïa region (Southern Algeria). *J Therm Eng* 2021;10:130-141. [\[Crossref\]](#)